

A Non-Conservative Stability Criterion for Networked Control Systems with time-varying Packet Delays

Martin Steinberger and Martin Horn

arXiv:2103.16514v1 [eess.SY] 30 Mar 2021

Abstract—A networked output feedback loop subject to packetized transmissions of the output signal is considered. Based on the small gain theorem, an easy-to-use stability criterion covering two important cases is presented. In the first case a packet numbering mechanism is employed whereas in the second case neither packet numbering nor synchronization between sender and receiver is assumed. The analysis makes use of acausal subsystems and deduces the optimal constant time delay that should be used in a nominal controller design such that additional packet delay variations introduced by the network are maximized. A simulation example of a networked control system with a filtered Smith predictor illustrates the application of the proposed criterion and compares the results to different approaches from literature.

Index Terms—Networked control systems, variable time delays, network delays, packetized transmissions, stability analysis, small gain theorem, acausal systems, filtered Smith predictor.

I. INTRODUCTION

The most fundamental question in the design and analysis of networked control systems (NCS) is how to guarantee closed loop stability under the presence of network imperfections, as pointed out, e.g., in [1]–[3]. Stability criteria based on Linear Matrix Inequalities (LMIs) are widespread in literature. They follow different ideas to prove stability of networked loops for a variable time delay that should be as large as possible. In addition, the number of variables in the LMIs should be as small as possible in order to reduce the computational complexity, see, for example, [4], [5] and references therein.

Different control design methods rest on the stability analysis. In [6], over-approximation techniques are used to design state controllers for loops with time-varying delays using LMI conditions. Sliding mode approaches are utilized in [7] together with a buffering mechanism to robustly stabilize spatially distributed networked feedback loops and render them insensitive to unknown bounded input disturbances. An alternative approach for the stability analysis is presented in [8]. It extends the small gain theorem (SGT) for feedback

Manuscript received ??, 2021; M. Steinberger and M. Horn were supported by the LEAD project “Dependable Internet of Things in Adverse Environments” funded by Graz University of Technology. The financial support by the Christian Doppler Research Association, the Austrian Federal Ministry for Digital and Economic Affairs and the National Foundation for Research, Technology and Development is gratefully acknowledged.

M. Steinberger and M. Horn are with the Institute of Automation and Control, Graz University of Technology, 8010 Graz, Austria (e-mail: martin.steinberger@tugraz.at; martin.horn@tugraz.at).

M. Horn is with the Christian Doppler Laboratory for Model Based Control of Complex Test Bed Systems, Institute of Automation and Control, Graz University of Technology, 8010 Graz, Austria.

loops with variable time delays. Surprisingly, stability is not always explicitly considered as, e.g., in [9], where an adaptive Smith predictor is applied to control an optical oven over the internet that is subject to variable time delays.

It is crucial for the stability analysis of networked loops with time-varying delays to also consider the packetized nature of network transmissions. This means, that, e.g., the measurement data is sent in separate packets over a transmission channel. Due to the fact that each packet may experience a different packet delay, the used packet skipping and hold mechanisms at the receiver side have to be taken into account, see [10]. This is an important step that is either implicitly considered as in [6] or not included in the analysis as, e.g., in [5] and [8].

The authors of [11] proposed a way how to include time-varying packet delays in the analysis by using a criterion based on the SGT. This work was extended in [12] to a network setup, where neither synchronization nor packet numbering is implemented. This allows to analyze feedback structures, where no packet reordering mechanism as, e.g., proposed in [13] is utilized. In [12], a robust stability criterion is presented as well, which allows to account for uncertain plant models in feedback loops with variable packet delays. However, the results from [11] and [12] might be conservative. Consequently, the contributions of the present paper are:

- (a) The existing SGT-based approaches are enhanced to get a less conservative stability criterion. This yields a larger range for the admissible time-varying packet delays.
- (b) A splitting of the considered NCS into a causal and an acausal subsystem is used to minimize the effect of the uncertain variable delay. This analysis also yields an optimal constant time delay for a nominal controller design.
- (c) The proposed computationally inexpensive criterion is applied to a networked loop consisting of an unstable plant and a filtered Smith predictor to underline the properties of the approach and compare the results to existing methods.

Notation: Entire sequences are written as $(y_k) = (y_0, y_1, y_2, \dots)$, one element is symbolized by y_k , where $k \in \mathbb{N}$ is the iteration index. $\|(y_k)\|_2$ is the 2-norm of sequence (y_k) . The z-transform of a sequence (y_k) is denoted as $\tilde{y}(z) = \mathcal{Z}\{(y_k)\}$. Discrete-time transfer functions $G(z)$ are written as functions of variable z . The infinity norm $\|G(z)\|_\infty$ is defined as the maximum of the corresponding magnitude plot of $G(z)$ that follows for $z = e^{j\omega h}$ and frequencies

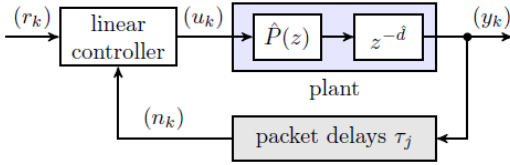


Fig. 1. Feedback loop that is closed by means of a communication network with variable time delays τ_j for the transmitted packets j .

$\omega \in [0, \pi/h]$, where h symbolizes the constant sampling time.

II. PROBLEM STATEMENT

The considered feedback loop consists of a plant, a packetized transmission network and a linear controller, see Fig. 1. The plant with input sequence (u_k) and output sequence (y_k) is given as

$$P(z) = \hat{P}(z)z^{-\hat{d}}, \quad (1)$$

where $\hat{P}(z)$ is a proper nominal discrete-time transfer function and $0 \leq \hat{d} \in \mathbb{N}$ represents a nominal plant delay. As a controller, one can, e.g., use $u(z) = C(z)(r(z) - n(z))$ as in [11] to get a unity feedback loop, or filtered Smith predictors as presented in [12].

Assumption 1 (Network delays): The elements of output sequence (y_k) are transmitted in separate packets j that are subject to individual bounded packet delays τ_j so that

$$0 \leq \underline{\tau}_N \leq \tau_j \leq \bar{\tau}_N \quad (2)$$

with $0 \leq \underline{\tau}_N < \bar{\tau}_N$ and $\underline{\tau}_N, \tau_j, \bar{\tau}_N \in \mathbb{N}$.

Please note that there are no further assumptions on the delay distribution nor on the maximal admissible change rate of two subsequent packet delays. The elements of output y_k are sent in individual packets j via the transmission channel to a receiver at the controller side (see Fig. 1) and may arrive at the same time instant or out of order due to the time-varying transmission delays. Hence, it is important to specify the used protocols, i.e. the packet selection and skipping mechanism as well as the hold mechanism that is active whenever no packet arrives at the receiver side. Two out of the three different protocols, formally introduced in [11] and [12], are considered in this work¹:

Protocol \mathcal{P}_1 : The most recent packet is used, if more packets are available at the same time. Packets are skipped, if they arrive after a more recent packet has already been received. This requires either a synchronization of sender and receiver or at least a numbering of subsequently sent packets.

Protocol \mathcal{P}_3 : Neither synchronization nor packet numbering is used. This represents the most reduced network transmission approach with the least possible overhead. Consequently, it constitutes the worst case for stability analysis as the order of arriving packets is unknown and any arriving packet may be selected at the receiver side.

Both protocols make use of a zero order hold mechanism on the receiver side. Compared to \mathcal{P}_1 and \mathcal{P}_3 , protocol \mathcal{P}_2

¹For the sake of compatibility, the same notation as in [12] is used in the present paper.

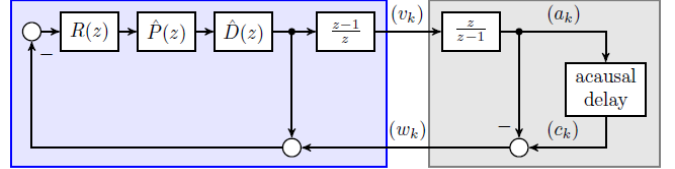


Fig. 2. Restructured feedback loop that is used for the stability analysis: nominal part (blue); uncertainty due to the (acausal) time-varying delays (gray).

presented in [11] is an intermediate case and is not considered here. In principle, the proposed stability criterion can also be formulated for \mathcal{P}_2 .

Combining plant delay (1) and network delay (2) results in a constant time delay $\hat{d} + \underline{\tau}_N$ and a time-varying delay that is bounded such that

$$0 \leq \tau_j - \underline{\tau}_N \leq \bar{\tau}_N - \underline{\tau}_N = \hat{\tau}_N. \quad (3)$$

For the nominal controller design and stability analysis presented below, an additional constant acausal time delay $0 \leq \tau_A \in \mathbb{N}$ is introduced, yielding a modified constant time delay

$$\hat{\tau} = \hat{d} + \underline{\tau}_N + \tau_A \quad (4)$$

and a (usually) acausal time-varying delay

$$-\tau_A \leq \tau_j - \underline{\tau}_N - \tau_A \leq \hat{\tau}_N - \tau_A \quad (5)$$

for the overall delay of plant and communication network. The specific choice of $\tau_A = 0$ constitutes the causal case as in [11], [12].

The goals of the present papers are: (i) derive less conservative stability conditions for protocols \mathcal{P}_1 and \mathcal{P}_3 compared to [11] and [12]; (ii) find an optimal choice τ_A^* for the acausal delay resulting in an increase of the admissible time-varying network delay $\hat{\tau}_N$ maintaining finite gain ℓ_2 stability of the closed loop.

III. STABILITY CRITERION

This section introduced the proposed stability criterion that rests on the separation of the original structure, presented in Fig 1, into a nominal part (blue in Fig. 2) and a part characterizing the uncertainty due to the time-varying packet delays (gray block in Fig. 2). In addition, the reference input (r_k) is zero and the remaining linear controller in Fig. 1 is represented by transfer function $R(z)$ with input sequence (n_k) , delayed measurement sequence (y_k) and output sequence (u_k) . A discrete-time integrator and differentiator are utilized to avoid issues for the case, where the nominal controller $R(z)$ is designed to achieve a dc-gain equal to one for the nominal loop, see [11] for details. The effect of the known constant time delay $\hat{\tau}$ (4) is included in the nominal (blue) part via transfer function

$$\hat{D}(z) = z^{-\hat{\tau}}. \quad (6)$$

Note that the acausal delay τ_A also appears in (6) because of (4). Before the following theorems are stated, some definitions are recalled. For more details see, e.g., [14].

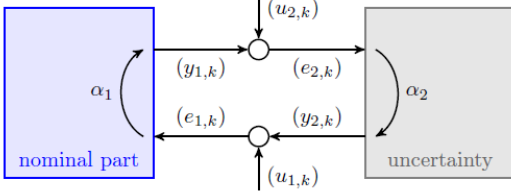


Fig. 3. Feedback loop for the formulation of the discrete-time small gain theorem. Either the nominal subsystem or the uncertainty might be acausal.

Definition 1 (Truncation of a sequence): The truncation of sequence $(f_k) : [a, \infty) \rightarrow \mathbb{R}$ at a finite time T is defined as

$$(f_k)_T = \begin{cases} 0 & \forall t \text{ if } T < a \\ f_k & a \leq k \leq T \\ 0 & k > T \geq a \end{cases}. \quad (7)$$

Definition 2 (Extended ℓ_2 space): A sequence (f_k) belongs to $\ell_2[a, \infty)$ if condition $\sum_{k=a}^{\infty} |f_k|^2 < \infty$ holds. The sequence $(f_k) \in \ell_{2e}[a, \infty)$, if its truncation belongs to $\ell_2[a, \infty)$, i.e. $(f_k)_T \in \ell_2[a, \infty)$ for all T .

Definition 3 (Finite gain ℓ_2 stability): A mapping $(y_k) = \mathcal{M}\{(u_k)\} : \ell_{2e}[a, \infty) \mapsto \ell_{2e}[a, \infty)$ is finite gain ℓ_2 stable if there exist constants $\alpha > 0$ and $\beta > 0$ such that

$$\|(y_k)\|_2 \leq \alpha \|(u_k)\|_2 + \beta \quad (8)$$

for $(u_k) \in \ell_2[a, \infty)$ and $(y_k) \in \ell_2[a, \infty)$, i.e. there is an affine bound of the norm of output sequence (y_k) . The constant α is referred to as the finite ℓ_2 gain.

Definition 4 (Causality): A mapping $(y_k) = \mathcal{M}\{(u_k)\} : \ell_{2e}[a, \infty) \mapsto \ell_{2e}[a, \infty)$ is causal if

$$(y_k)_T = (\mathcal{M}\{(u_k)\})_T = (\mathcal{M}\{(u_k)_T\})_T \quad (9)$$

for all finite $T > 0$ and $(u_k) \in \ell_{2e}[a, \infty)$.

Please note that there are definitions of the finite ℓ_2 gain that are different to [14]. In [15], the ℓ_2 gain is defined for causal mappings, i.e. it is a combination of Definition 3 and 4 using the truncation operator such that $\|(y_k)_T\|_2 \leq \alpha \|(u_k)_T\|_2 + \beta$ for $(u_k) \in \ell_{2e}[a, \infty)$.

Based on [16] where an SGT for continuous-time systems with acausal subsystems is introduced, we can now state the discrete-time SGT for the feedback loop shown in Fig. 3 with $(u_{1,k}), (u_{2,k}) \in \ell_2[a, \infty)$ and $(e_{1,k}), (e_{2,k}), (y_{1,k}), (y_{2,k}) \in \ell_{2e}[a, \infty)$. The nominal part and the uncertainty are characterized by mappings $(y_{1,k}) = \mathcal{M}_1\{(e_{1,k})\}$ and $(y_{2,k}) = \mathcal{M}_2\{(e_{2,k})\}$ respectively. They are assumed to be finite gain ℓ_2 stable, i.e.

$$\|(y_{1,k})\| \leq \alpha_1 \|(e_{1,k})\| + \beta_1 \quad \forall (e_{1,k}) \in \ell_2[a, \infty), \quad (10a)$$

$$\|(y_{2,k})\| \leq \alpha_2 \|(e_{2,k})\| + \beta_2 \quad \forall (e_{2,k}) \in \ell_2[a, \infty). \quad (10b)$$

If both mappings are causal, the classical SGT as stated in [14], [15] can be applied. However, for the stability analysis of networked control systems as considered in this paper, it will turn out to be beneficial that one subsystem is acausal.

k	-2	-1	0	1	2	3	4	5	6	7	8	9	10	11	12	13	14	15	16
$b_k^{(2)}$	1	2	3	4	5	6	7	8	9	10	11	11	11	11	11	11	11	11	
$b_k^{(1)}$	0	1	2	3	4	5	6	7	8	9	10	11	11	11	11	11	11	11	
$b_k^{(0)} = a_k$	0	0	1	2	3	4	5	6	7	8	9	10	11	11	11	11	11	11	
$b_k^{(1)}$	0	0	0	1	2	3	4	5	6	7	8	9	10	11	11	11	11	11	

Fig. 4. Packets on the way for $\hat{\tau}_N = 3$, $\bar{v} = 1$ and $\tau_A = 2$. Darker colors represent more recent packets.

Theorem 1 (Acausal SGT for discrete-time systems): Consider the feedback loop shown Fig. 3 with finite ℓ_2 gains (10). Let

$$\alpha_1 \alpha_2 < 1 \quad (11)$$

and conditions

$$(\mathcal{M}_1\{\mathcal{M}_2\{(e_{2,k})\}\})_T = (\mathcal{M}_1\{\mathcal{M}_2\{(e_{2,k})_T\}\})_T \quad (12a)$$

$$(\mathcal{M}_2\{\mathcal{M}_1\{(e_{1,k})\}\})_T = (\mathcal{M}_2\{\mathcal{M}_1\{(e_{1,k})_T\}\})_T \quad (12b)$$

$$\begin{aligned} & \left\| (\mathcal{M}_\nu\{(e_{\nu,k}^{(1)}) + (e_{\nu,k}^{(2)})\})_T \right\|_2 \leq \\ & \left\| (\mathcal{M}_\nu\{(e_{\nu,k}^{(1)})_T\})_T \right\|_2 + \left\| (\mathcal{M}_\nu\{(e_{\nu,k}^{(2)})_T\})_T \right\|_2, \end{aligned} \quad (12c)$$

hold for all $(e_{\nu,k}), (e_{\nu,k}^{(1)}), (e_{\nu,k}^{(2)}) \in \ell_{2e}[a, \infty)$ and $\nu \in \{1, 2\}$. Then, the closed loop system is finite gain ℓ_2 stable.

Proof: The proof directly follows as discrete-time counterpart of the continuous-time version from [16] evaluated for $n_1 = n_2 = 1$ and $a_1 = a_2 = a$. ■

Remark 1: Conditions (12a) and (12b) ensure, that the cascade connection of \mathcal{M}_1 and \mathcal{M}_2 (and vice versa) are causal. For example, $(y_{1,k}) = \mathcal{M}_1\{(e_{1,k})\} = \mathcal{M}_1\{(u_{1,k}) + (y_{2,k})\} = \mathcal{M}_1\{(u_{1,k}) + \mathcal{M}_2\{(e_{2,k})\}\}$ has to be causal according to Definition 4 for $(u_{1,k})$ identically to zero as claimed in (12a).

Remark 2: Please note that condition (12c) is automatically fulfilled if both subsystems in Fig. 3 are linear.

Theorem 1 establishes the basis for the proposed stability criterion for feedback loops as depicted in Fig. 1. The nominal part with input (w_k) and output (v_k) in Fig. 2 can be described by transfer function

$$M(z) = \frac{-R(z)\hat{P}(z)\hat{D}(z)}{1 + R(z)\hat{P}(z)\hat{D}(z)} \frac{(z-1)}{z} \quad (13)$$

with the corresponding finite ℓ_2 gain of $\alpha_1 = \|M(z)\|_\infty$. In contrast, it is more challenging to find the ℓ_2 gain $\alpha_2 = \alpha$ of the uncertainty in Fig. 2. This is because (acausal) time-varying packet delays in combination with protocol \mathcal{P}_1 or \mathcal{P}_3 have to be considered. Hence, we follow the general procedure proposed in [11], [12] and extend it to include the acausal delay τ_A . To find the ℓ_2 gain α associated with the uncertainty, one has to maximize the norm of output $w_k = c_k - a_k$, where a_k is the summation of input sequence $(v_k)_T = (v_0, v_1, v_2, \dots, v_T, 0, \dots) = (\bar{v}, \bar{v}, \bar{v}, \dots, \bar{v}, 0, \dots)$ with constant \bar{v} and truncation time $T > 0$. As a result, sequence $(a_k) = (a_0, a_1, a_2, \dots, a_T, a_{T+1}, \dots) = (\bar{v}, 2\bar{v}, 3\bar{v}, \dots, (T+1)\bar{v}, (T+1)\bar{v}, \dots)$ is transmitted and experiences time-varying delays bounded as stated in (5). Figure 4 shows all possible packets on the way for $\hat{\tau}_N = 3$ and an acausal delay of $\tau_A = 2$. This means that, e.g., the packet containing $a_5 = 6$ might

TABLE I

OPTIMAL ACAUSAL DELAYS τ_A^* AND RELATED ℓ_2 GAINS $\alpha^* = g(\tau_A^*, \hat{\tau}_N)$ FOR DIFFERENT MAXIMAL ADMISSIBLE VARIABLE NETWORK DELAYS $\hat{\tau}_N$ AND PROTOCOL \mathcal{P}_3 .

$\hat{\tau}_N$	α^*	τ_A^*									
1	1.0000	1	11	10.000	10	21	19.000	19	31	28.031	28
2	2.0000	2	12	11.000	11	22	20.000	20	32	29.000	29
3	2.7839	2	13	11.955	11	23	21.000	21	33	30.000	30
4	3.6878	3	14	12.845	12	24	21.904	21	34	30.950	30
5	4.6260	4	15	13.734	13	25	22.784	22	35	31.826	31
6	5.5377	5	16	14.614	14	26	23.659	23	36	32.699	32
7	6.4254	6	17	15.488	15	27	24.531	24	37	33.574	33
8	7.3095	7	18	16.369	16	28	25.411	25	38	34.451	34
9	8.2082	8	19	17.250	17	29	26.288	26	39	35.325	35
10	9.0921	9	20	18.125	18	30	27.16	27	40	36.196	36

arrive at the receiver side at time instants $k \in \{3, 4, 5, 6\}$ as can be seen in Fig. 4 (red packets labeled with number 6). The set of all packets that might arrive at time instant k is $\{b_k^{(-\tau_A)}, b_k^{(-\tau_A+1)}, \dots, b_k^{(\hat{\tau}_N-\tau_A)}\}$. Depending on the actual protocol, e.g., the most recent packet is selected as c_k and further used. Consequently, the ℓ_2 gain of the uncertainty is

$$\alpha = \sup_{T>0} \alpha_T \quad \text{with} \quad \alpha_T = \sqrt{\frac{\|((w_k)_T)\|_2^2}{\|((v_k)_T)\|_2^2}}, \quad (14)$$

and $\|((v_k)_T)\|_2^2 = (1+T)\bar{v}^2$. Please note that α depends on τ_A , which will be chosen to minimize the finite ℓ_2 gain.

Table I shows the optimal acausal delays τ_A^* that yield a minimization of the related gain for different maximal delays $\hat{\tau}_N$ and protocol \mathcal{P}_3 . Details on the calculations can be found in Appendix A. With this, we are able to state the main stability criterion for the considered NCS.

Theorem 2 (Stability criterion for NCS using acausal subsystems): Consider the networked feedback loop shown in Fig. 1 with plant (1) and a packetized transmission network subject to network delays (2). Let the linear controller $u(z) = -R(z)n(z)$ for $(r_k) = 0 \forall k$ be designed for a nominal delay $\hat{\tau} = \hat{d} + \underline{\tau}_N + \tau_A^*$ and suppose that acausal delay τ_A^* and the corresponding finite ℓ_2 gain α^* are given such that

(a) for protocol \mathcal{P}_1 (skip old packets, take newest if more packets are available):

$$\tau_A^* = \left\lceil \frac{\bar{\tau}_N + \underline{\tau}_N}{2} \right\rceil \quad \text{or} \quad \tau_A^* = \left\lfloor \frac{\bar{\tau}_N + \underline{\tau}_N}{2} \right\rfloor, \quad (15a)$$

$$\alpha^* = \alpha_{\mathcal{P}_1}^* = \max \{ \tau_A^*, \hat{\tau}_N - \tau_A^* \} \quad (15b)$$

(b) for protocol \mathcal{P}_3 (no numbering nor synchronization, worst case)

$$\alpha^* = \alpha_{\mathcal{P}_3}^* = g(\tau_A^*, \hat{\tau}_N) \quad (16)$$

in accordance with the Table I.

The feedback loop is finite gain ℓ_2 stable for all bounded time-varying packet delays $0 \leq \underline{\tau}_N \leq \tau_j \leq \bar{\tau}_N$, if

$$\left\| M(z) \right\|_{\infty} \alpha^* = \left\| \frac{R(z)\hat{P}(z)}{1+R(z)\hat{P}(z)\hat{D}(z)} \frac{(z-1)}{z} \right\|_{\infty} \alpha^* < 1 \quad (17)$$

is fulfilled. Constant τ_A^* is the optimal acausal time delay that minimizes the finite ℓ_2 gain α^* for a given $\hat{\tau}_N$.

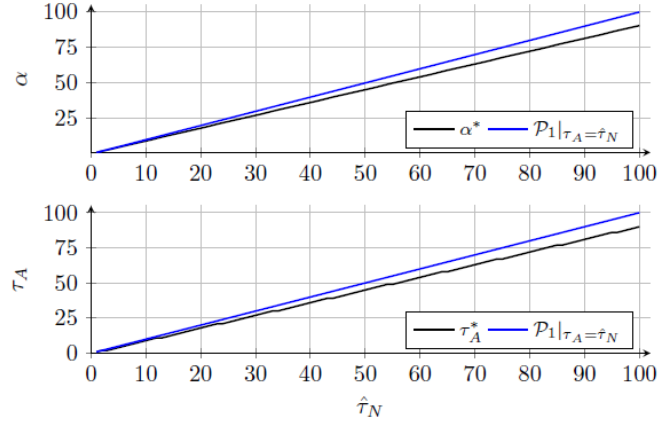


Fig. 5. Optimal acausal time delay τ_A^* and gain α^* for protocol \mathcal{P}_3 (black) and a possible over-estimation (blue).

Proof: A proof is given in Appendix A. ■

Remark 3: Note that relation (16) cannot be stated explicitly, as it is also visible in Table I. The steps, how to numerically find optimal values τ_A^* and α^* , are detailed in Appendix A. However, it is possible to over-estimate the non-linear characteristics in Table I using results from protocol \mathcal{P}_1 so that

$$\tau_A = \hat{\tau}_N \quad \text{and} \quad \alpha = \alpha_{\mathcal{P}_1} \Big|_{\tau_A = \hat{\tau}_N} = \hat{\tau}_N \quad (18)$$

hold for protocol \mathcal{P}_3 as depicted in Fig. 5. The specific patterns of packet delays leading to the ℓ_2 gains for both protocols are presented in the Appendix.

Remark 4: For the causal case, i.e. for $\tau_A = 0$, one obtains the same conditions as (i) in [11] for a unity feedback loop closed via a network channel, where $R(z) = C(z)$, $\hat{d} = 0$, $\underline{\tau}_N = 0$ and, as a result, $\hat{D}(z) = 1$ (no delay in plant); (ii) in [12] for a NCS with a filtered Smith predictor, $R(z) = \frac{C(z)F(z)}{1+C(z)H(z)}$, $H(z) = \hat{P}(z)(1-\hat{D}(z)F(z))$ and $\hat{d} \geq 0$, $\underline{\tau}_N \geq 0$, which implies $\hat{D}(z) = z^{-\hat{\tau}} = z^{-\hat{d}-\underline{\tau}_N}$.

Remark 5: Theorem 2 can be extended in a straightforward way to uncertain plant models $P(z) = \hat{P}(z)z^{-\hat{d}}(1+\delta P)$ as presented in [12] for the causal case.

IV. SIMULATION EXAMPLE

The application of Theorem 2 is shown for an NCS consisting of a filtered Smith predictor and the unstable plant

$$P(z) = \frac{0.0051271}{z-1.051} z^{-5} \quad (19)$$

as used in [12] for the causal case with sampling time $h = 1$. The nominal controller $C(z)$ with prefilter $V(z)$ in the form of $u(z) = C(z)(V(z)r(z) - n(z))$ is designed such that the delay-free, nominal closed loop has poles at $p_1 = p_2 = 0.95$ and the overshoot during set-point changes is reduced by $V(z)$. This results in, transfer functions

$$C(z) = \frac{29.504(z-0.9835)}{z-1}, \quad V(z) = \frac{0.041317(z-0.6)}{(z-0.9835)} \quad (20)$$

The pole of filter transfer function $F(z)$ for the predictor is fixed at $p = 0.95$, see [12] for details. Since a filtered Smith

TABLE II

EXAMPLE: MAXIMAL ADMISSIBLE VARIABLE TIME DELAY $\hat{\tau}_N$ FOR CONVENTIONAL LMI APPROACHES AND SGT APPROACHES THAT INCLUDE THE PACKETIZED NATURE OF NETWORK TRANSMISSIONS.

approach	theorem	max. $\hat{\tau}_N$
LMI	Theorem 1(i) [12] ([5])	5
LMI	Theorem 1(ii) [12] ([5])	1
SGT	Theorem 2 \mathcal{P}_1 [12]	4
SGT	Theorem 2 \mathcal{P}_3 [12]	2
SGT acausal	Theorem 2 \mathcal{P}_1	6
SGT acausal	Theorem 2 \mathcal{P}_3	3

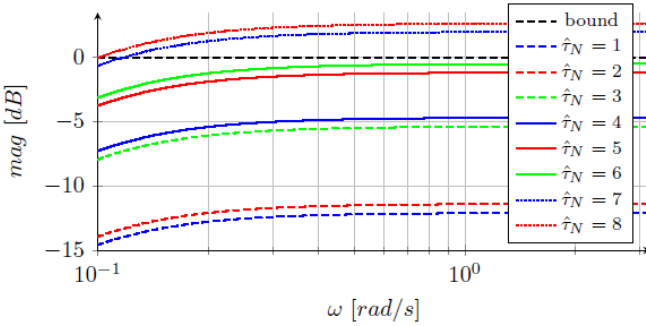


Fig. 6. Example: magnitude plots for $M(z)\alpha^*$ using protocol \mathcal{P}_1 and different maximal network delays $\hat{\tau}_N$.

predictor structure is considered, the nominal design does not depend on τ_A . However, τ_A is taken into account in the overall constant delay (4) for the predictor.

Evaluation of the LMI conditions stated in [12] that are based on [5], yields either 5 or 1 for the maximal admissible time-varying delay $\hat{\tau}_N$, see also Table II. However, as shown in [12], there are sequences of packet delays that already lead to instability for $\hat{\tau}_N = 4$. This is because the packetized character of the transmissions is not explicitly considered in the analysis. This issue is overcome by using Theorem 2 from [12], where the SGT is utilized for the causal case. The maximum achievable $\hat{\tau}_N$ is 4 for protocol \mathcal{P}_1 and 2 for \mathcal{P}_3 .

Next, Theorem 2 is evaluated for the example. Conditions (15), and (16) are evaluated for $\tau_N = 0$ and different $\hat{\tau}_N$. The optimal acausal delay τ_A^* is used in the predictor and relation (17) is checked by using bode magnitude plots for $M(z)\alpha^*$ as shown in Fig. 6 and 7. Figure 6 reveals that one can show stability for a maximal value of $\hat{\tau}_N = 6$ with the proposed theorem for \mathcal{P}_1 , which is larger than using the LMI-based approach.

A maximum $\hat{\tau}_N$ of 3 is achieved for protocol \mathcal{P}_3 as depicted in Fig. 7. Please note that one can find delay patterns [12] for $\hat{\tau}_N = 4$ that lead to instability. Hence, the upper bound provided by Theorem 2 equals the largest achievable value for the admissible time-varying delay. Over-estimation (18) for \mathcal{P}_3 will often lead to a smaller admissible $\hat{\tau}_N$, which is not the case for the presented example, see green dashed line in Fig. 7. Table II presents a comparison of the results for all considered approaches for the simulation example.

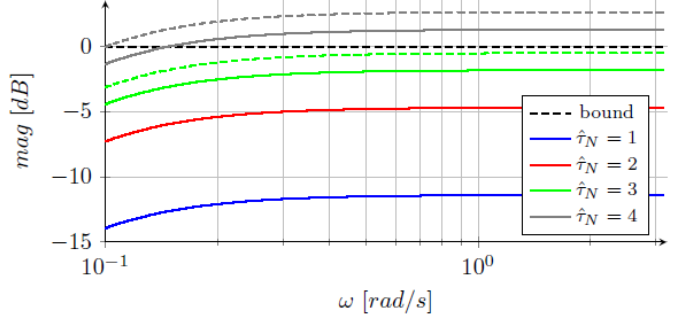


Fig. 7. Example: magnitude plots for $M(z)\alpha^*$ using protocol \mathcal{P}_3 and different maximal network delays $\hat{\tau}_N$. Dotted lines represent results obtained by using the over-estimated values (18).

V. CONCLUSION

A stability criterion based on a SGT for feedback loops with acausal subsystems is proposed that allows to achieve less conservative results compared to existing approaches in literature. It allows to show stability for a larger admissible variable time delay introduced by a communication network. Since packets containing measurement data are sent in separate packets over the transmission channel, it is vital to also include the packetized nature of the transmissions. This is possible by using an extension of the SGT for discrete-time systems (Theorem 1), where one subsystem might be acausal. The acausality of one subsystem is exploited to maximize the achievable delay $\hat{\tau}_N$ for different protocols (Theorem 2). Additionally, the proposed approach yields an optimal acausal delay τ_A^* that is used to design the nominal controller for the constant delay $\hat{d} + \tau_N + \tau_A^*$.

A simulation example for a NSC with filtered Smith predictor provides insights to the application of this easy-to-use criterion for networked loops and compares the results to LMI-based solutions, where the packet selection and hold mechanisms at the receiver side cannot be directly included.

APPENDIX A PROOF OF THEOREM 2

The proof is based on the application of Theorem 1 to the feedback structure shown in Fig. 2. Hence, the gain of the nominal part and the uncertainty due to the time-varying delays are considered. Gain α_1 , as defined in (10a), is given by $\alpha_1 = \|M(z)\|_\infty$, where (13) is used for the description of the nominal part. Condition (12c) is fulfilled for the considered NCS because both subsystems (nominal part and uncertainty) are linear, see also Remark 1. Since Fig. 1 is equivalent to Fig. 2 for $(r_k) = (0, 0, \dots)$, the cascade connections of both subsystems are causal, as claimed by (12a) and (12b). Consequently, only the calculation of the finite ℓ_2 gain $\alpha^* = \alpha_2$ for the uncertainty remains to show (15b), (16), (17) in Theorem 2. This is done below for the gray subsystem in Fig. 2 with input v_k (with $\bar{v} = 1$) and output w_k considering protocols \mathcal{P}_1 and \mathcal{P}_3 .

Fig. 8. Packet pattern and inner signals of the uncertainty for \mathcal{P}_1 , $\hat{\tau}_N = 3$, $T = 10$ and $\tau_A = 2$

A. Protocol \mathcal{P}_1

Figure 8 shows all inner signals as well as the output w_k of the uncertainty for a maximal admissible variable time delay $\hat{\tau}_N = 3$ and an additional acausal delay $\tau_A = 2$. The input sequence (v_k) and (a_k) , are truncated at $T = 10$, as shown in Section III. To maximize the norm of w_k , all possible packets on the way $\{b_k^{(-\tau_A)}, b_k^{(-\tau_A+1)}, \dots, b_k^{(\hat{\tau}_N-\tau_A)}\}$ (see also Fig. 4) are considered. For example at time instant $k = 0$, the packet containing 3 yields the largest absolute value for $w_k = b_k^{(-2)} - a_k$. Consequently, $a_2 = 3$ has to arrive at time instant $k = 0$, i.e. two time instants before it is sent. Its corresponding packet delay is $\tau_3 = -2$. In addition, one has to take into account the fact, that each packet can only be received once at the receiver side and, as defined for protocol \mathcal{P}_1 , the most recent packet is chosen if more packets are available. The packet received at the last time instant, i.e. c_{k-1} , is used if no packet is received at instant k . Figure 8 presents the resulting packet pattern that results in a maximization of the norm of (w_k) . The worst case delay pattern is $\tau_j = -2$ for all j . Figure 9 extends the analysis to different $\hat{\tau}_N$, T and acausal delays τ_A , where also the minimal delay $-\tau_A$ and maximal delay $\hat{\tau}_N - \tau_A$ are indicated. All resulting delay patterns and output sequences show a similar structure as for the causal case [11], with the important differences that: (i) a maximal relative delay

$$\bar{\tau} = \max \{ -\tau_A, \hat{\tau}_N - \tau_A \} \quad (21)$$

is relevant; (ii) the norm of the output sequence for the introductory part A (green), main part B (yellow) and remaining part C (red) is given by $\|((w_k)_T)\|_2^2 = A + B + C = 2A + B$,

$$\left\| (w_k)_T \right\|_2^2 = 2 \sum_{i=1}^{\bar{\tau}-1} i^2 \bar{v}^2 + (T - \bar{\tau} + 2) \bar{\tau}^2 \bar{v}^2 \quad (22)$$

for $T - \bar{\tau} + 2 > 0$, i.e. $T > \bar{\tau} - 2$.

Evaluating (14) with (22) yields α_T as depicted in Fig. 10 for different acausal delays τ_A (blue plus signs). The black circles are the resulting worst case gains found numerically by direct variation of all possible combinations of packet delays τ_j . Hence, one can mathematically reproduce the true worst case gains α_T that tend to $\alpha = \bar{\tau}$ for $T \rightarrow \infty$, see dashed lines in Fig. 10. An alternative way to plot the results from Fig. 10 is presented in Fig. 11, where circles indicate the different values for α_T for different T and the blue solid line visualizes α as a function of τ_A . As a consequence, the optimal choice for the

r_1	m_1	m_2	k	-4	-3	-2	-1	0	1	2	3	4	5	6	7	8	9	10	11	12	13	14	15	16	17	18
2	0	r_2 w_2	2	2	2	2	2	2	2	2	2	2	2	2	2	2	2	2	2	2	2	2	2	2	2	2
			0	0	-1	-2	-2	-2	-2	-2	-2	-2	-2	-2	-2	-2	-2	-2	-2	-2	-1	0	0	0	0	
2	-1	r_2 w_2	1	1	1	1	1	1	1	1	1	1	1	1	1	1	1	1	1	1	1	1	1	1	1	1
			0	0	-1	-1	-1	-1	-1	-1	-1	-1	-1	-1	-1	-1	-1	-1	-1	-1	-1	-1	0	0	0	
2	-2	r_2 w_2	2	2	2	2	2	2	2	2	2	2	2	2	2	2	2	2	2	2	2	2	2	2	2	2
			1	2	3	2	3	2	3	2	3	2	3	2	3	2	3	2	3	2	3	1	0	0	0	
3	0	r_2 w_2	3	3	3	3	3	3	3	3	3	3	3	3	3	3	3	3	3	3	3	3	3	3	3	3
			0	0	0	-1	-3	-3	-3	-3	-3	-3	-3	-3	-3	-3	-3	-3	-3	-3	-2	-1	0	0	0	
3	-1	r_2 w_2	2	2	2	2	2	2	2	2	2	2	2	2	2	2	2	2	2	2	2	2	2	2	2	2
			0	0	-1	-2	-3	-2	-3	-2	-3	-2	-3	-2	-3	-2	-3	-2	-3	-2	-1	0	0	0	0	
3	-2	r_2 w_2	1	2	3	2	3	2	3	2	3	2	3	2	3	2	3	2	3	2	3	1	0	0	0	0
			0	1	2	3	2	3	2	3	2	3	2	3	2	3	2	3	2	3	1	0	0	0	0	
3	-3	r_2 w_2	3	3	3	3	3	3	3	3	3	3	3	3	3	3	3	3	3	3	3	3	3	3	3	3
			0	1	2	3	3	3	3	3	3	3	3	3	3	3	3	3	3	3	3	2	1	0	0	0
4	0	r_2 w_2	4	4	4	4	4	4	4	4	4	4	4	4	4	4	4	4	4	4	4	4	4	4	4	4
			0	0	0	-1	-2	-3	-4	-4	-4	-4	-4	-4	-4	-4	-4	-4	-4	-4	-3	-2	-1	0	0	
4	-1	r_2 w_2	3	3	3	3	3	3	3	3	3	3	3	3	3	3	3	3	3	3	3	3	3	3	3	3
			0	0	0	1	2	3	3	3	3	3	3	3	3	3	3	3	3	3	3	2	1	0	0	
4	-2	r_2 w_2	2	2	2	2	2	2	2	2	2	2	2	2	2	2	2	2	2	2	2	2	2	2	2	2
			0	0	0	-1	-2	-2	-2	-2	-2	-2	-2	-2	-2	-2	-2	-2	-2	-2	-1	0	0	0	0	
4	-3	r_2 w_2	3	3	3	3	3	3	3	3	3	3	3	3	3	3	3	3	3	3	3	3	3	3	3	3
			0	1	2	3	3	3	3	3	3	3	3	3	3	3	3	3	3	3	3	2	1	0	0	0
4	-4	r_2 w_2	4	4	4	4	4	4	4	4	4	4	4	4	4	4	4	4	4	4	4	4	4	4	4	4
			1	2	3	4	4	4	4	4	4	4	4	4	4	4	4	4	4	4	3	2	1	0	0	0
5	0	r_2 w_2	5	5	5	5	5	5	5	5	5	5	5	5	5	5	5	5	5	5	5	5	5	5	5	5
			0	0	0	-1	-2	-3	-4	-4	-4	-4	-4	-4	-4	-4	-4	-4	-4	-4	-4	-3	-2	-1	0	0
5	-1	r_2 w_2	4	4	4	4	4	4	4	4	4	4	4	4	4	4	4	4	4	4	4	4	4	4	4	4
			0	0	-1	-1	-1	-1	-1	-1	-1	-1	-1	-1	-1	-1	-1	-1	-1	-1	-1	0	0	0	0	
5	-2	r_2 w_2	3	3	3	3	3	3	3	3	3	3	3	3	3	3	3	3	3	3	3	3	3	3	3	3
			0	0	0	-1	-2	-2	-2	-2	-2	-2	-2	-2	-2	-2	-2	-2	-2	-2	-2	-1	0	0	0	
5	-3	r_2 w_2	2	2	2	2	2	2	2	2	2	2	2	2	2	2	2	2	2	2	2	2	2	2	2	2
			0	1	2	3	3	3	3	3	3	3	3	3	3	3	3	3	3	3	3	2	1	0	0	
5	-4	r_2 w_2	3	3	3	3	3	3	3	3	3	3	3	3	3	3	3	3	3	3	3	3	3	3	3	3
			0	1	2	3	4	4	4	4	4	4	4	4	4	4	4	4	4	4	4	4	4	4	4	
5	-5	r_2 w_2	5	5	5	5	5	5	5	5	5	5	5	5	5	5	5	5	5	5	5	5	5	5	5	5
			0	0	0	-1	-2	-3	-4	-4	-4	-4	-4	-4	-4	-4	-4	-4	-4	-4	-4	-3	-2	-1	0	0

Fig. 9. Resulting delay patterns (τ_j) and worst case output sequences (w_k) for \mathcal{P}_1 , $\hat{\tau}_N \in \{2, 3, 4\}$, $T = 10$ (top), $T = 5$ (middle), and $T = 2$ (bottom).

acausal delay (black dots) is (15a) and α^* equal to (15), see Theorem 2. The resulting worst case delay pattern is

$$\tau_j = \begin{cases} \bar{\tau}^* & \text{if } \bar{\tau}^* = \hat{\tau}_N - \tau_A \\ -\bar{\tau}^* & \text{otherwise} \end{cases} . \quad (23)$$

B. Protocol \mathcal{P}_3

The calculation of α^* is more demanding for protocol \mathcal{P}_3 , because the delay patterns from the previous section only partially reproduce gains α_T , e.g., for \mathcal{P}_3 and $\tau_A = \hat{\tau}_N$. This is visualized in Fig. 18 using blue plus signs. An analysis of the delay patterns that correspond to the numerically found worst case gains α_T reveals that three different delay patterns \mathcal{P}'_3 , \mathcal{P}''_3 and \mathcal{P}'''_3 have to be considered to mathematically describe the gains related to protocol \mathcal{P}_3 .

1) *Delay Pattern \mathcal{P}'_3* : The first packet arrival pattern is based on [12] for the causal case of \mathcal{P}_3 . Figure 12 show the associated delay pattern, inner signals of the uncertainty and the worst case output sequence for $\hat{\tau}_N = 3$, $T = 10$ and $\tau_A = 2$. This is then generalized for different $\hat{\tau}_N$, T , and τ_A as shown in Fig. 13 for $\hat{\tau}_N \in \{2, 3, 4\}$ and $T \in \{2, 5, 10\}$. Hence, delay pattern

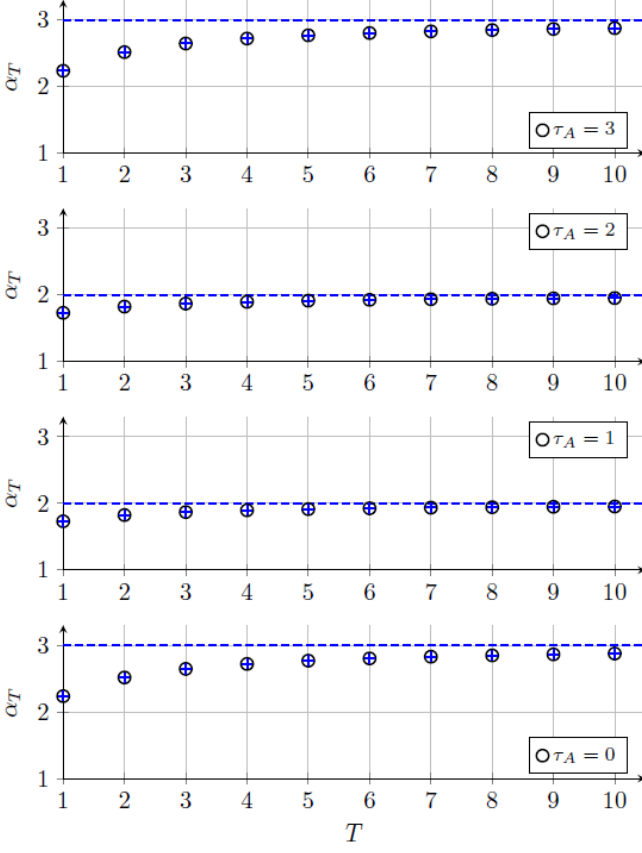


Fig. 10. Gains as a function of truncation point T and the acausal delay τ_A for \mathcal{P}_1 and $\hat{\tau}_N = 3$.

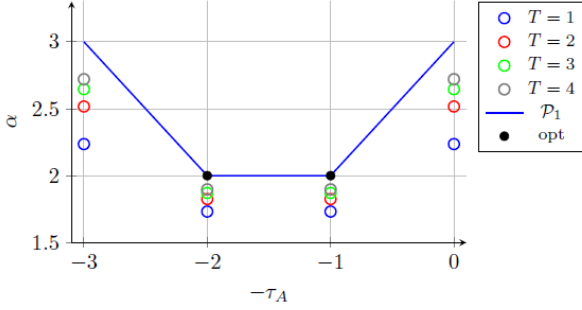


Fig. 11. Gains as function of the acausal delay for \mathcal{P}_1 and $\hat{\tau}_N = 3$.

k	-2	-1	0	1	2	3	4	5	6	7	8	9	10	11	12	13	14	15	16
$b_k^{(-3)} - a_k$	1	2	2	2	2	2	2	2	2	2	2	1	0	0	0	0	0	0	
$b_k^{(-1)} - a_k$	0	1	1	1	1	1	1	1	1	1	1	0	0	0	0	0	0	0	
$b_k^{(0)} - a_k$	0	0	0	0	0	0	0	0	0	0	0	0	0	0	0	0	0	0	
$b_k^{(1)} - a_k$	0	0	-1	-1	-1	-1	-1	-1	-1	-1	-1	0	0	0	0	0	0	0	
$b_k^{(-3)}$	1	2	3	4	5	6	7	8	9	10	11	12	13	14	15	16	17	18	
$b_k^{(-1)}$	0	1	2	3	4	5	6	7	8	9	10	11	12	13	14	15	16	17	
$b_k^{(0)}$	0	0	1	2	3	4	5	6	7	8	9	10	11	12	13	14	15	16	
$b_k^{(1)}$	0	0	0	1	2	3	4	5	6	7	8	9	10	11	12	13	14	15	
c_k	0	0	0	1	1	1	1	5	5	5	9	9	9	9	11	11	11	11	
packet arr.	no	no	no	yes	no	no	no	yes	no	no	no	yes	no	no	no	no	no	no	
w_k	0	0	-1	-2	-3	-4	-1	-2	-3	-4	-1	-2	-2	0	0	0	0	0	
block	A	B	B	B	B	B	B	B	B	B	C	C	C	C	C	C	C	C	
τ_j	1	0	-1	-2	1	0	-1	-2	1	0	-1	-2	1	0	-1	-2	1	0	

Fig. 12. Packet pattern and inner signals of the uncertainty for \mathcal{P}'_3 , $\hat{\tau}_N = 3$, $T = 10$ and $\tau_A = 2$.

$$(\tau_j) = (\underbrace{(\hat{\tau}_N - \tau_A), (\hat{\tau}_N - \tau_A - 1), \dots, -\tau_A}_*, \star, \star, \dots) \quad (24)$$

τ_N	min	max	k	-4	-3	-2	-1	0	1	2	3	4	5	6	7	8	9	10	11	12	13	14	15	16	17	18
2	0	2	τ_j	0	0	1	2	-2	-3	-4	-2	-3	-4	-3	-4	-1	1	1	0	0	2	1	0	3	1	
2	-1	1	τ_j	0	0	0	-1	-1	-1	-1	-1	-1	-1	-1	-1	-1	-1	-1	-1	-1	0	0	1	0	1	
2	-2	0	τ_j	0	0	0	0	-1	-2	0	-1	-2	0	-1	-2	0	0	-1	-2	0	0	-1	-2	0	0	
3	0	3	τ_j	3	2	1	0	3	2	1	0	3	2	1	0	3	2	1	0	3	2	1	0	3	1	
3	-1	2	τ_j	0	0	0	-1	-2	-3	-4	-5	-6	-7	-8	-9	-10	-11	-12	-13	-14	-15	-16	-17	-18		
3	-2	1	τ_j	0	0	0	0	-1	-2	-3	-4	-5	-6	-7	-8	-9	-10	-11	-12	-13	-14	-15	-16	-17		
3	-3	0	τ_j	0	0	0	0	-1	-2	-3	-4	-5	-6	-7	-8	-9	-10	-11	-12	-13	-14	-15	-16	-17		
4	0	4	τ_j	4	3	2	1	0	4	3	2	1	0	4	3	2	1	0	4	3	2	1	0	4	1	
4	-1	3	τ_j	0	0	0	0	-1	-2	-3	-4	-5	-6	-7	-8	-9	-10	-11	-12	-13	-14	-15	-16	-17		
4	-2	2	τ_j	0	0	0	0	-1	-2	-3	-4	-5	-6	-7	-8	-9	-10	-11	-12	-13	-14	-15	-16	-17		
4	-3	1	τ_j	0	0	0	0	-1	-2	-3	-4	-5	-6	-7	-8	-9	-10	-11	-12	-13	-14	-15	-16	-17		
4	-4	0	τ_j	0	0	0	0	-1	-2	-3	-4	-5	-6	-7	-8	-9	-10	-11	-12	-13	-14	-15	-16	-17		
5	0	5	τ_j	5	4	3	2	1	0	5	4	3	2	1	0	5	4	3	2	1	0	5	4	3		
5	-1	4	τ_j	0	0	0	0	-1	-2	-3	-4	-5	-6	-7	-8	-9	-10	-11	-12	-13	-14	-15	-16	-17		
5	-2	3	τ_j	0	0	0	0	-1	-2	-3	-4	-5	-6	-7	-8	-9	-10	-11	-12	-13	-14	-15	-16	-17		
5	-3	2	τ_j	0	0	0	0	-1	-2	-3	-4	-5	-6	-7	-8	-9	-10	-11	-12	-13	-14	-15	-16	-17		
5	-4	1	τ_j	0	0	0	0	-1	-2	-3	-4	-5	-6	-7	-8	-9	-10	-11	-12	-13	-14	-15	-16	-17		
5	-5	0	τ_j	0	0	0	0	-1	-2	-3	-4	-5	-6	-7	-8	-9	-10	-11	-12	-13	-14	-15	-16	-17		
6	0	6	τ_j	6	5	4	3	2	1	0	6	5	4	3	2	1	0	6	5	4	3	2	1	0		
6	-1	5	τ_j	0	0	0	0	-1	-2	-3	-4	-5	-6	-7	-8	-9	-10	-11	-12	-13	-14	-15	-16	-17		
6	-2	4	τ_j	0	0	0	0	-1	-2	-3	-4	-5	-6	-7	-8	-9	-10	-11	-12	-13	-14	-15	-16	-17		
6	-3	3	τ_j	0	0	0	0	-1	-2	-3	-4	-5	-6	-7	-8	-9	-10	-11	-12	-13	-14	-15	-16	-17		
6	-4	2	τ_j	0	0	0	0	-1	-2	-3	-4	-5	-6	-7	-8	-9	-10	-11	-12	-13	-14	-15	-16	-17		
6	-5	1	τ_j	0	0	0	0	-1	-2	-3	-4	-5	-6	-7	-8	-9	-10	-11	-12	-13	-14	-15	-16	-17		
6	-6	0	τ_j	0	0	0	0	-1	-2	-3	-4	-5	-6	-7	-8	-9	-10	-11	-12	-13	-14	-15	-16	-17		

Fig. 13. Resulting delay patterns (τ_j) and worst case output sequences (w_k) for \mathcal{P}'_3 , $\hat{\tau}_N \in \{2, 3, 4\}$, $T = 10$ (top), $T = 5$ (middle), and $T = 2$ (bottom).

yields $\| (w_k)_T \|_2^2 = A + B + C + D$ consisting of four parts A, B, C and D. Introductory part A consists of $\hat{\tau}_N - \tau_A$ samples. It contributes to $\| (w_k)_T \|_2^2$ with

$$A = \sum_{i=1}^{\hat{\tau}_N - \tau_A} \left(\min \{i, T+1\} \right)^2 \bar{v}^2 \quad (25)$$

and $T \geq 0$, where this formulation with the min-operator is used to account for cases where $T+1 < \hat{\tau}_N$ as, e.g., shown in the Fig. 13 for $T = 2$, $\hat{\tau}_N = 4$ and $\tau_A = 0$. Block B consists of k_1 (yellow) blocks of length $\hat{\tau}_N + 1$, containing a repeating sequence $(\hat{\tau}_N - \tau_A, \hat{\tau}_N - \tau_A + 1, \dots, 2\hat{\tau}_N - \tau_A)$ with a squared norm of

$$d = \sum_{i=0}^{\hat{\tau}_N} \left(\hat{\tau}_N - \tau_A + i \right)^2 \bar{v}^2 \quad (26)$$

The causal case in [12] provides the basis to generalize the calculation of k_1 for the acausal one. Overall $T + 2\hat{\tau}_N + 1$ are taken into account in the analysis, where block B contribute with $\hat{\tau}_N - \tau_A$ samples. To get k_1 , one subtracts the length of the repeating sequence $(\hat{\tau}_N + 1)$ from the remaining $T + 1 + \hat{\tau}_N + \tau_A$ samples so many times that $\leq 3\hat{\tau}_N$ samples are left.

The remaining samples $k_2 = T + 1 + \hat{\tau}_N + \tau_A - k_1(\hat{\tau}_N + 1)$ are split into

$$k_3 = \left\lfloor \frac{k_2}{\hat{\tau}_N + 1} \right\rfloor \quad (27)$$

times $\hat{\tau}_N + 1$ samples (block C, blue) and the left $k_2 - k_3(\hat{\tau}_N + 1)$ samples shown in red. This yield

$$\| (w_k)_T \|_2 = \underbrace{\sum_{i=1}^{\hat{\tau}_N - \tau_A} i^2 \bar{v}^2}_{A} + \underbrace{k_1 \sum_{i=0}^{\hat{\tau}_N} (\hat{\tau}_N - \tau_A + i)^2 \bar{v}^2}_{B} + \quad (28)$$

$$\sum_{j=k_1}^{k_1+k_3-1} \left\{ \underbrace{\sum_{i=\hat{\tau}_N - \tau_A + j(\hat{\tau}_N + 1)}^{2\hat{\tau}_N - \tau_A + j(\hat{\tau}_N + 1)} (a_i - a_{j(\hat{\tau}_N + 1)})^2}_{C} + \right. \\ \left. \underbrace{\sum_{i=\hat{\tau}_N - \tau_A + (k_1+k_3)(\hat{\tau}_N + 1)}^{T+2\hat{\tau}_N} (a_i - a_{\hat{\tau}_N - \tau_A + (k_1+k_3)(\hat{\tau}_N + 1)})^2}_{D} \right\}$$

which is used in the calculation of α_T . The ℓ_2 gain follows from (14), (26), (28) and

$$\alpha_T^2 = \frac{A + \frac{T+1}{\hat{\tau}_N+1} d + C + D}{1+T} = \frac{A + C + D}{1+T} + \frac{d}{\hat{\tau}_N+1} \quad (29)$$

for $T \rightarrow \infty$ such that

$$d = \sum_{i=1}^{\hat{\tau}_N} (\Delta\tau - 1 + i)^2 \bar{v}^2 \quad (30) \\ = \left[(\Delta\tau - 1)^2 \sum_{i=1}^{\hat{\tau}_N+1} 1 + 2(\Delta\tau - 1) \sum_{i=1}^{\hat{\tau}_N+1} i + \sum_{i=1}^{\hat{\tau}_N+1} i^2 \right] \bar{v}^2 \\ = (\hat{\tau}_N + 1) \left[\Delta\tau^2 + \Delta\tau \hat{\tau}_N + \frac{1}{3} \hat{\tau}_N^2 + \frac{1}{6} \hat{\tau}_N \right] \bar{v}^2$$

with $\Delta\tau = \hat{\tau}_N - \tau_A$ and so

$$\alpha_{\mathcal{P}'_3} = \sqrt{\Delta\tau^2 + \Delta\tau \hat{\tau}_N + \frac{1}{3} \hat{\tau}_N^2 + \frac{1}{6} \hat{\tau}_N} \quad (31)$$

Figure 18 shows the results for α_T and the corresponding ℓ_2 gains $\alpha_{\mathcal{P}'_3}$ for different acausal delays. Condition (31) reduces to $\alpha = \sqrt{\frac{\bar{\tau}}{6}(14\bar{\tau} + 1)}$ in causal case where $\Delta\tau = \hat{\tau}_N = \bar{\tau}$, see [12]. The presented delay pattern allows to reproduce additional points in Fig. 18 as, e.g., for $\tau_A = 0$ and $\tau_A = 1$.

2) *Delay Pattern \mathcal{P}''_3 :* A second delay pattern follows by modifying the introductory part of \mathcal{P}'_3 such that

$$(\tau_j) = ((\hat{\tau}_N - \tau_A), \underbrace{-\tau_A, -\tau_A, \dots, -\tau_A}_{\hat{\tau}_N \text{ times}}, \quad (32) \\ \underbrace{(\hat{\tau}_N - \tau_A), (\hat{\tau}_N - \tau_A - 1), \dots, -\tau_A, \star, \star, \dots}_{\star})$$

The resulting packet patterns and inner signals of the uncertainty are exemplified in Fig. 14 for $\hat{\tau}_N = 3$, $T = 10$ and an acausal delay of $\tau_A = 2$. Figure 15 illustrate the patterns for different $\hat{\tau}_N$, τ_A and truncations T . In contrast to (28), the introductory part A is split into A^+ for $k \geq 0$ and A^- for $k < 0$. All other parts remain the same as in \mathcal{P}'_3 . According

k	-2	-1	0	1	2	3	4	5	6	7	8	9	10	11	12	13	14	15	16
$b_3^{(-2)} - a_k$	1	2	2	2	2	2	2	2	2	2	2	1	0	0	0	0	0	0	
$b_3^{(-1)} - a_k$	0	1	1	1	1	1	1	1	1	1	1	1	1	0	0	0	0	0	
$b_3^0 - a_k$	0	0	0	0	0	0	0	0	0	0	0	0	0	0	0	0	0	0	
$b_3^{(1)} - a_k$	0	0	0	0	0	0	0	0	0	0	0	0	0	0	0	0	0	0	
$b_3^{(2)} - a_k$	1	2	3	4	5	6	7	8	9	10	11	12	13	14	15	16	17	18	
$b_3^{(3)} - a_k$	0	1	2	3	4	5	6	7	8	9	10	11	12	13	14	15	16	17	
$b_3^{(4)} - a_k$	0	1	2	3	4	5	6	7	8	9	10	11	12	13	14	15	16	17	
$b_3^{(5)} - a_k$	0	1	2	3	4	5	6	7	8	9	10	11	12	13	14	15	16	17	
$b_3^{(6)} - a_k$	0	1	2	3	4	5	6	7	8	9	10	11	12	13	14	15	16	17	
$b_3^{(7)} - a_k$	0	1	2	3	4	5	6	7	8	9	10	11	12	13	14	15	16	17	
$b_3^{(8)} - a_k$	0	1	2	3	4	5	6	7	8	9	10	11	12	13	14	15	16	17	
$b_3^{(9)} - a_k$	0	1	2	3	4	5	6	7	8	9	10	11	12	13	14	15	16	17	
$b_3^{(10)} - a_k$	0	1	2	3	4	5	6	7	8	9	10	11	12	13	14	15	16	17	
$b_3^{(11)} - a_k$	0	1	2	3	4	5	6	7	8	9	10	11	12	13	14	15	16	17	
$b_3^{(12)} - a_k$	0	1	2	3	4	5	6	7	8	9	10	11	12	13	14	15	16	17	
$b_3^{(13)} - a_k$	0	1	2	3	4	5	6	7	8	9	10	11	12	13	14	15	16	17	
$b_3^{(14)} - a_k$	0	1	2	3	4	5	6	7	8	9	10	11	12	13	14	15	16	17	
$b_3^{(15)} - a_k$	0	1	2	3	4	5	6	7	8	9	10	11	12	13	14	15	16	17	
$b_3^{(16)} - a_k$	0	1	2	3	4	5	6	7	8	9	10	11	12	13	14	15	16	17	
$b_3^{(17)} - a_k$	0	1	2	3	4	5	6	7	8	9	10	11	12	13	14	15	16	17	
$b_3^{(18)} - a_k$	0	1	2	3	4	5	6	7	8	9	10	11	12	13	14	15	16	17	
$b_3^{(19)} - a_k$	0	1	2	3	4	5	6	7	8	9	10	11	12	13	14	15	16	17	
$b_3^{(20)} - a_k$	0	1	2	3	4	5	6	7	8	9	10	11	12	13	14	15	16	17	
$b_3^{(21)} - a_k$	0	1	2	3	4	5	6	7	8	9	10	11	12	13	14	15	16	17	
$b_3^{(22)} - a_k$	0	1	2	3	4	5	6	7	8	9	10	11	12	13	14	15	16	17	
$b_3^{(23)} - a_k$	0	1	2	3	4	5	6	7	8	9	10	11	12	13	14	15	16	17	
$b_3^{(24)} - a_k$	0	1	2	3	4	5	6	7	8	9	10	11	12	13	14	15	16	17	
$b_3^{(25)} - a_k$	0	1	2	3	4	5	6	7	8	9	10	11	12	13	14	15	16	17	
$b_3^{(26)} - a_k$	0	1	2	3	4	5	6	7	8	9	10	11	12	13	14	15	16	17	
$b_3^{(27)} - a_k$	0	1	2	3	4	5	6	7	8	9	10	11	12	13	14	15	16	17	
$b_3^{(28)} - a_k$	0	1	2	3	4	5	6	7	8	9	10	11	12	13	14	15	16	17	
$b_3^{(29)} - a_k$	0	1	2	3	4	5	6	7	8	9	10	11	12	13	14	15	16	17	
$b_3^{(30)} - a_k$	0	1	2	3	4	5	6	7	8	9	10	11	12	13	14	15	16	17	
$b_3^{(31)} - a_k$	0	1	2	3	4	5	6	7	8	9	10	11	12	13	14	15	16	17	
$b_3^{(32)} - a_k$	0	1	2	3	4	5	6	7	8	9	10	11	12	13	14	15	16	17	
$b_3^{(33)} - a_k$	0	1	2	3	4	5	6	7	8	9	10	11	12	13	14	15	16	17	
$b_3^{(34)} - a_k$	0	1	2	3	4	5	6	7	8	9	10	11	12	13	14	15	16	17	
$b_3^{(35)} - a_k$	0	1	2	3	4	5	6	7	8	9	10	11	12	13	14	15	16	17	
$b_3^{(36)} - a_k$	0	1	2	3	4	5	6	7	8	9	10	11	12	13	14	15	16	17	
$b_3^{(37)} - a_k$	0	1	2	3	4	5	6	7	8	9	10	11	12	13	14	15	16	17	
$b_3^{(38)} - a_k$	0	1	2	3	4	5	6	7	8	9	10	11	12	13	14	15	16	17	
$b_3^{(39)} - a_k$	0	1	2	3	4	5	6	7	8	9	10	11	12	13	14	15	16	17	
$b_3^{(40)} - a_k$	0	1	2	3	4	5	6	7	8	9	10	11	12	13	14	15	16	17	
$b_3^{(41)} - a_k$	0	1	2	3	4	5	6	7	8	9	10	11	12	13	14	15	16	17	
$b_3^{(42)} - a_k$	0	1	2	3	4	5	6	7	8	9	10	11	12	13	14	15	16	17	
$b_3^{(43)} - a_k$	0	1	2	3	4	5	6	7	8	9	10	11	12	13	14	15	16	17	
$b_3^{(44)} - a_k$	0	1	2	3	4	5	6	7	8	9	10	11	12	13	14	15	16	17	
$b_3^{(45)} - a_k$	0	1	2	3	4	5	6	7	8	9	10	11	12	13	14	15	16	17	
$b_3^{(46)} - a_k$	0	1	2	3	4	5	6	7	8	9	10	11	12	13	14	15	16	17	
$b_3^{(47)} - a_k$	0	1	2	3	4	5	6	7	8	9	10	11	12	13	14	15	16	17	
$b_3^{(48)} - a_k$	0	1	2	3	4	5	6	7	8	9	10	11	12	13	14	15	16	17	
$b_3^{(49)} - a_k$	0	1	2	3	4	5	6	7	8	9	10	11	12	13	14	15	16	17	
$b_3^{(50)} - a_k$	0	1	2	3	4	5	6	7	8	9	10	11	12	13	14	15	16	17	
$b_3^{(51)} - a_k$	0	1	2	3	4	5	6	7	8	9	10	11	12	13	14	15	16	17	
$b_3^{(52)} - a_k$	0	1	2	3	4	5	6	7	8	9	10	11	12	13	14	15	16	17	
$b_3^{(53)} - a_k$	0	1	2	3	4	5	6	7	8	9	10	11	12	13	14	15	16	17	
$b_3^{(54)} - a_k$	0	1	2	3	4	5	6	7	8	9	10	11	12	13	14	15	16	17	
$b_3^{(55)} - a_k$	0	1	2	3	4	5	6	7	8	9	10	11	12	13	14	15	16	17	
$b_3^{(56)} - a_k$	0	1	2	3	4	5	6	7	8	9	10	11	12	13	14	15	16	17	
$b_3^{(57)} - a_k$	0	1	2	3	4	5	6	7	8	9	10	11	12	13	14	15	16	17	
$b_3^{(58)} - a_k$	0	1	2	3	4	5	6	7	8	9	10	11	12	13	14	15	16	17	
$b_3^{(59)} - a_k$	0	1	2	3	4	5	6	7	8	9	10	11	12	13	14	15	16	17	
$b_3^{(60)} - a_k$	0	1	2	3	4	5	6	7	8	9	10	11	12	13	14	15	16	17	
$b_3^{(61)} - a_k$	0	1	2	3	4	5	6	7	8	9	10	11	12	13	14	15	16	17	
$b_3^{(62)} - a_k$	0	1	2	3	4	5	6	7	8	9	10	11	12	13	14	15	16	17	

k	-2	-1	0	1	2	3	4	5	6	7	8	9	10	11	12	13	14	15	16
$b_k^{(2)} - a_k$	1	2	2	2	2	2	2	2	2	2	1	0	0	0	0	0	0	0	
$b_k^{(-1)} - a_k$	0	1	1	1	1	1	1	1	1	1	1	1	0	0	0	0	0	0	
$b_k^{(0)} - a_k$	0	0	0	0	0	0	0	0	0	0	0	0	0	0	0	0	0	0	
$b_k^{(1)} - a_k$	0	0	-1	-1	-1	-1	-1	-1	-1	-1	-1	0	0	0	0	0	0	0	
$b_k^{(-2)}$	1	2	3	4	5	6	7	8	9	10	11	12	13	14	15	16	17	18	
$b_k^{(-1)}$	0	1	2	3	4	5	6	7	8	9	10	11	12	13	14	15	16	17	
$b_k^{(0)}$	0	0	1	2	3	4	5	6	7	8	9	10	11	12	13	14	15	16	
$b_k^{(1)}$	0	0	0	1	2	3	4	5	6	7	8	9	10	11	12	13	14	15	
c_k	1	2	3	4	5	6	7	8	9	10	11	9	9	9	11	11	11	11	
packet arr.	yes	no	yes	yes	no	no	no	yes	yes	yes	yes								
w_k	1	2	2	2	2	2	2	2	1	2	2	-1	-2	-2	0	0	0	0	
block	A	B	B	B	B	B	B	B	C	C	D	D	D	D	D	D	D	D	
τ_j	-2	-2	-2	-2	-2	-2	-2	-2	-2	-2	-2	1	1	1	1	1	1	1	

Fig. 16. Packet pattern and inner signals of the uncertainty for \mathcal{P}_3''' , $\hat{\tau}_N = 3$, $T = 10$ and $\tau_A = 2$.

$$A^- = \begin{cases} 0 & \text{if } \tau_A \in \{0, 1\} \\ \sum_{i=2}^{\tau_A} \left(\min \{i, T+1\} \right)^2 \bar{v}^2 & \text{otherwise} \end{cases} \quad (33b)$$

Relation (14) in combination with (28) and (33) allows to calculate α_T as presented in Fig. 18. It can be observed that the limit of α_T for $T \rightarrow \infty$ is equal to \mathcal{P}_3' . However, larger values

$$\alpha_{\mathcal{P}_3''} = \sup_T \alpha_{T, \mathcal{P}_3''} \quad (34)$$

result for smaller T , as, e.g. for $\tau_A = 2$ and $T = 3$ in Fig. 18.

3) *Delay Pattern \mathcal{P}_3''' :* Almost all points in Fig. 18 can be mathematically described by using either \mathcal{P}_1 , \mathcal{P}_3' or \mathcal{P}_3'' . However, this is not true for, e.g., $\tau_A = 3$ and $T = 3$. Thus, the additional delay pattern

$$(\tau_j) = \left(\underbrace{-\tau_A, -\tau_A, \dots, -\tau_A}_{T-\hat{\tau}_N+1 \text{ elements}}, (\hat{\tau}_N - \tau_A), \underbrace{-\tau_A, -\tau_A, \dots, -\tau_A}_{\hat{\tau}_N \text{ elements}}, (\hat{\tau}_N - \tau_A), (\hat{\tau}_N - \tau_A), \dots \right) \quad (35)$$

for $T - \hat{\tau}_N + 1 \geq 0$, i.e. $T \geq \hat{\tau}_N - 1$ is utilized. The corresponding patterns and inner signals are shown in Fig. 16 and 17 and for different values of $\hat{\tau}_N$, τ_A , and T . Block A, C and D consist of $\hat{\tau}_N - 1$, $\hat{\tau}_N$ and $\hat{\tau}_N + 1$ samples, respectively. As a result, the length of (yellow) block B is $T - \hat{\tau}_N - \tau_A + 2$. The worst case norm of output sequence (w_k) for \mathcal{P}_3''' is given by

$$\|w_k\|_{2,T}^2 = A + B + C + D \quad (36)$$

with

$$A = \begin{cases} 0 & \text{if } \tau_A \in \{0, 1\} \\ \sum_{i=1}^{\tau_A-1} \left(i - \delta^{(i)} \right)^2 \bar{v}^2 & \text{otherwise} \end{cases} \quad (37a)$$

τ_N	min	max	k	-4	-3	-2	-1	0	1	2	3	4	5	6	7	8	9	10	11	12	13	14	15	16	17	18	
2	0	2	τ_j	0	0	0	0	0	0	0	0	0	0	0	0	0	0	0	2	2	2	2	2	2	2	2	
2	-1	1	τ_j	0	1	1	1	1	1	1	1	1	1	1	1	1	1	1	1	1	1	1	1	1	1	1	
2	-2	0	τ_j	0	2	2	2	2	2	2	2	2	2	2	2	2	2	2	2	2	2	2	2	2	2	2	
3	-3	0	τ_j	0	0	0	0	0	0	0	0	0	0	0	0	0	0	0	0	0	0	0	0	0	0	0	
3	-2	1	τ_j	0	0	0	0	0	0	0	0	0	0	0	0	0	0	0	0	0	0	0	0	0	0	0	
3	-1	2	τ_j	0	1	2	2	2	2	2	2	2	2	2	2	2	2	2	2	2	2	2	2	2	2	2	
3	0	3	τ_j	0	1	2	3	2	2	2	2	2	2	2	2	2	2	2	2	2	2	2	2	2	2	2	
4	-4	0	τ_j	0	0	0	0	0	0	0	0	0	0	0	0	0	0	0	0	0	0	0	0	0	0	0	
4	-3	1	τ_j	0	0	0	0	0	0	0	0	0	0	0	0	0	0	0	0	0	0	0	0	0	0	0	
4	-2	2	τ_j	0	0	0	0	1	2	2	2	2	2	2	2	2	2	2	2	2	2	2	2	2	2	2	
4	-1	3	τ_j	0	0	0	0	1	2	3	2	3	3	3	3	3	3	3	3	3	3	3	3	3	3	3	
4	0	4	τ_j	0	0	0	0	1	2	3	4	3	4	4	4	4	4	4	4	4	4	4	4	4	4	4	
7	τ_N	min	max	k	-4	-3	-2	-1	0	1	2	3	4	5	6	7	8	9	10	11	12	13	14	15	16	17	18
2	0	2	τ_j	0	0	0	0	0	0	0	0	0	0	0	0	0	0	0	0	0	0	0	0	0	0	0	0
2	-1	1	τ_j	0	1	1	1	1	1	1	1	1	1	1	1	1	1	1	1	1	1	1	1	1	1	1	1
2	-2	0	τ_j	0	2	2	2	2	2	2	2	2	2	2	2	2	2	2	2	2	2	2	2	2	2	2	2
3	-3	0	τ_j	0	0	0	0	0	0	0	0	0	0	0	0	0	0	0	0	0	0	0	0	0	0	0	0
3	-2	1	τ_j	0	0	0	0	1	2	1	1	1	1	1	1	1	1	1	1	1	1	1	1	1	1	1	1
3	-1	2	τ_j	0	0	0	1	2	1	2	2	1	2	2	2	2	2	2	2	2	2	2	2	2	2	2	2
3	0	3	τ_j	0	0	0	1	2	3	2	3	3	2	3	3	3	3	3	3	3	3	3	3	3	3	3	3
4	-4	0	τ_j	0	0	0	0	0	0	0	0	0	0	0	0	0	0	0	0	0	0	0	0	0	0	0	0
4	-3	1	τ_j	0	0	0	0	1	0	1	1	1	1	1	1	1	1	1	1	1	1	1	1	1	1	1	1
4	-2	2	τ_j	0	0	0	0	1	2	1	2	2	2	2	2	2	2	2	2	2	2	2	2	2	2	2	2
4	-1	3	τ_j	0	0	0	1	2	3	2	3	3	3	3	3	3	3	3	3	3	3	3	3	3	3	3	3
4	0	4	τ_j	0	0	0	1	2	3	4	3	4	4	4	4	4	4	4	4	4	4	4	4	4	4	4	4
7	τ_N	min	max	k	-4	-3	-2	-1	0	1	2	3	4	5	6	7	8	9	10	11	12	13	14	15	16	17	18
2	0	2	τ_j	0	0	0	0	0	0	0	0	0	0	0	0	0	0	0	0	0	0	0	0	0	0	0	0
2	-1	1	τ_j	0	1	1	1	1	1	1	1	1	1	1	1	1	1	1	1	1	1	1	1	1	1	1	1
2	-2	0	τ_j	0	2	2	2	2	2	2	2	2	2	2	2	2	2	2	2	2	2	2	2	2	2	2	2
3	-3	0	τ_j	0	0	0	0	0	0	0	0	0	0	0	0	0	0	0	0	0	0	0	0	0	0	0	0
3	-2	1	τ_j	0	0	0	0	1	2	1	1	1	1	1	1	1	1	1	1	1	1	1	1	1	1	1	1
3	-1	2	τ_j	0	0	0	0	1	2	2	2	2	2	2	2	2	2	2	2	2	2	2	2	2	2	2	2
3	0	3	τ_j	0	0	0	0	1	2	3	2	3	3	3	3	3	3	3	3	3	3	3	3	3	3	3	3
4	-4	0	τ_j	0	0	0	0	0	0	0	0	0	0	0	0	0	0	0	0	0	0	0	0	0	0	0	0
4	-3	1	τ_j	0	0	0	0	0	1	2	1	1	1	1	1	1	1	1	1	1	1	1	1	1	1	1	1
4	-2	2	τ_j	0	0	0	0	1	2	2	2	2	2	2	2	2	2	2	2	2	2	2	2	2	2	2	2
4	-1	3	τ_j	0	0	0	0	1	2	3	2	3	3	3	3	3	3	3	3	3	3	3	3	3	3	3	3
4	0	4	τ_j	0	0	0	0	1	2	3	4	3	4	4	4	4	4	4	4	4	4	4	4	4	4	4	4

$$B = \begin{cases} (T - \hat{\tau}_N - \tau_A + 2) \tau_A^2 \bar{v}^2 & \text{if } T \geq \hat{\tau}_N - 2 + \tau_A \\ (T - \tau_A + 2) \tau_A^2 \bar{v}^2 & \text{otherwise} \end{cases} \quad (37c)$$

$$C = \begin{cases} \sum_{i=\tau_A-1}^{\tau_A+\hat{\tau}_N-2} \left(\min \{i, \tau_A\} \right)^2 \bar{v}^2 & \text{if } T \geq \hat{\tau}_N - 2 + \tau_A \\ 0 & \text{otherwise} \end{cases} \quad (37d)$$

$$D = \sum_{i=\hat{\tau}_N-\tau_A}^{2\hat{\tau}_N-\tau_A} \left(\min \{i, \hat{\tau}_N - 1\} \right)^2 \bar{v}^2 \quad (37e)$$

for $T \geq \max\{\hat{\tau}_N - 1\}$. The different cases in (37) allow to correctly calculate $\alpha_{T, \mathcal{P}_3''}$ also for small truncation T as shown in Fig. 17 as well as

$$\alpha_{\mathcal{P}_3''} = \sup_T \alpha_{T, \mathcal{P}_3''} . \quad (38)$$

4) *Protocol \mathcal{P}_3 :* To find the overall finite ℓ_2 gain for protocol \mathcal{P}_3 one has to combine $\mathcal{P}_$

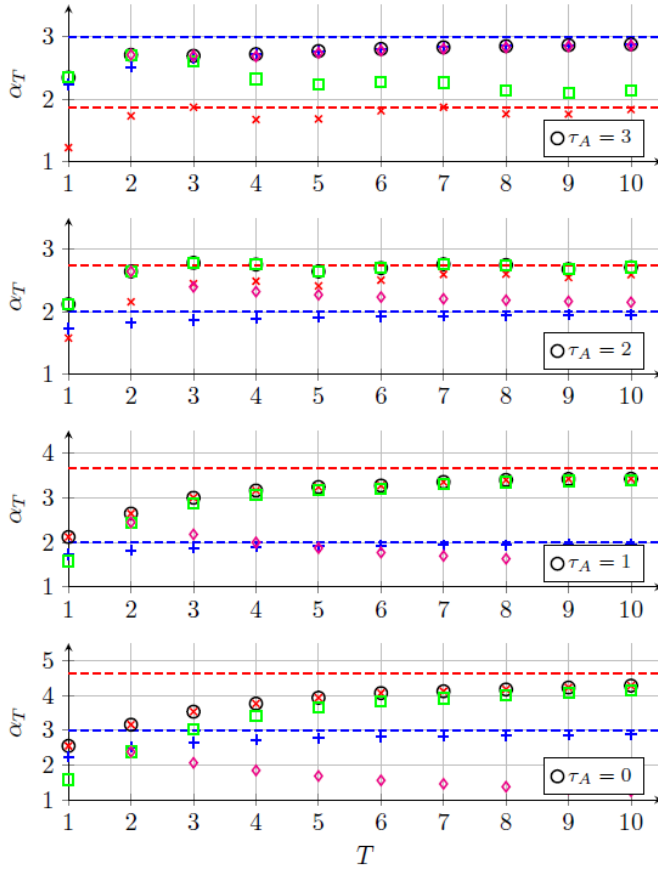


Fig. 18. Gains as a function of truncation point T and the acausal delay τ_A for $\hat{\tau}_N = 3$ and \mathcal{P}_1 (blue), \mathcal{P}_3' (red), \mathcal{P}_3'' (green), \mathcal{P}_3''' (magenta).

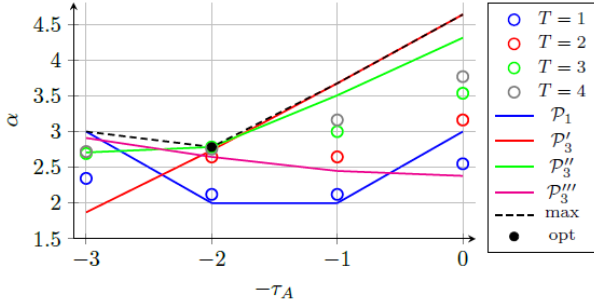


Fig. 19. Gains as a function of the acausal delay for \mathcal{P}_3 and $\hat{\tau}_N = 3$

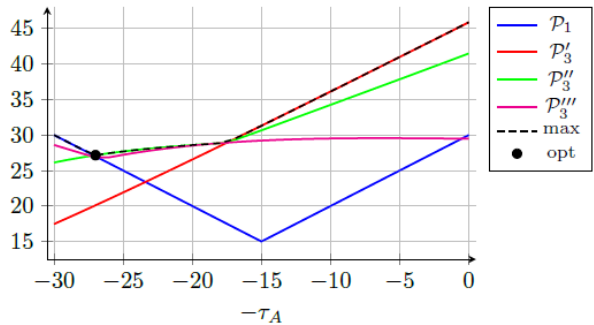


Fig. 20. Gains as a function of the acausal delay for \mathcal{P}_3 and $\hat{\tau}_N = 30$

Different gains that depend on the actual choice of the acausal delay τ_A follow for the considered delay patterns. Values for α_T that are found by direct variation all possible combinations of packet delays τ_j are indicated as black circles in Fig. 18 to show that the used mathematical description exactly reproduces all α_T . In Fig. 19, the results for $T = \{1, 2, 3, 4\}$ are shown depending on acausal delay τ_A . Results for larger T are omitted for clarity in the plot. The optimal ℓ_2 gain α^* and the optimal acausal delay τ_A^* are found numerically as the minimum among the different patterns (black dots in Fig. 19 and 20) such that

$$\alpha^* = \min_{\tau_A} \left\{ \max_{\tau_A} \left\{ \alpha_{\mathcal{P}_1}, \alpha_{\mathcal{P}_3'}, \alpha_{\mathcal{P}_3''}, \alpha_{\mathcal{P}_3'''} \right\} \right\}, \quad (39)$$

with the corresponding optimal choice for the acausal delay

$$\tau_A^* = \operatorname{argmin}_{\tau_A} \left\{ \max_{\tau_A} \left\{ \alpha_{\mathcal{P}_1}, \alpha_{\mathcal{P}_3'}, \alpha_{\mathcal{P}_3''}, \alpha_{\mathcal{P}_3'''} \right\} \right\}. \quad (40)$$

The numeric evaluation of (39), (40) results in relation (16) in Theorem 2 and Table I.

As pointed out in Remark 3, it is possible to make use of the gain that follows for \mathcal{P}_1 evaluated at $\tau_A = \hat{\tau}_N$ as an over-estimation of α^* for protocol \mathcal{P}_3 , cf. Fig 19 and 20.

REFERENCES

- [1] P. Park, S. C. Ergen, C. Fischione, C. Lu, and K. H. Johansson, "Wireless Network Design for Control Systems: A Survey," *IEEE Communications Surveys and Tutorials*, vol. 20, no. 2, pp. 978–1013, 2018.
- [2] D. Zhang, P. Shi, Q.-G. Wang, and L. Yu, "Analysis and synthesis of networked control systems: A survey of recent advances and challenges," *ISA Transactions*, vol. 66, pp. 376–392, 2017.
- [3] R. A. Gupta and M.-Y. Chow, "Networked Control System: Overview and Research Trends," *IEEE Transactions on Industrial Electronics*, vol. 57, no. 7, pp. 2527–2535, 2010.
- [4] A. Seuret, F. Gouaisbaut, and E. Fridman, "Stability of discrete-time systems with time-varying delays via a novel summation inequality," *IEEE Transactions on Automatic Control*, vol. 60, no. 10, pp. 2740–2745, 2015.
- [5] X. Li and H. Gao, "A new model transformation of discrete-time systems with time-varying delay and its application to stability analysis," *IEEE Transactions on Automatic Control*, vol. 56, no. 9, pp. 2172–2178, 2011.
- [6] M. Cloosterman, L. Hetel, N. van de Wouw, W. Heemels, J. Daafouz, and H. Nijmeijer, "Controller synthesis for networked control systems," *Automatica*, vol. 46, no. 10, pp. 1584 – 1594, 2010.
- [7] J. Ludwiger, M. Steinberger, and M. Horn, "Spatially distributed networked sliding mode control," *IEEE Control Systems Letters*, vol. 3, no. 4, pp. 972–977, 2019.
- [8] C.-Y. Kao and B. Lincoln, "Simple stability criteria for systems with time-varying delays," *Automatica*, vol. 40, no. 8, pp. 1429 – 1434, 2004.
- [9] A. P. Batista and P. G. Jota, "Performance improvement of an NCS closed over the internet with an adaptive Smith Predictor," *Control Engineering Practice*, vol. 71, pp. 34–43, 2018.
- [10] M. Steinberger, M. Tranninger, M. Horn, and K. H. Johansson, "How to simulate networked control systems with variable time delays?" in *21st IFAC World Congress*, Berlin, 2020.
- [11] M. Steinberger and M. Horn, "A stability criterion for networked control systems with packetized transmissions," *IEEE Control Systems Letters*, vol. 5, no. 3, pp. 911 – 916, 2021.
- [12] ———, "From classical to networked control: Retrofitting the concept of smith predictors," *arXiv:2010.05486*, 2020.
- [13] A. Liu, W.-a. Zhang, L. Yu, S. Liu, and M. Z. Q. Chen, "New results on stabilization of networked control systems with packet disordering," *Automatica*, vol. 52, pp. 255–259, 2015.
- [14] M. Vidyasagar, *Nonlinear Systems Analysis*. SIAM: Society for Industrial and Applied Mathematics, 2002.
- [15] S. Sastry, *Nonlinear Systems: Analysis, Stability and Control*. Springer New York, 1999.
- [16] H. U. Ünal and A. Iftar, "A small gain theorem for systems with non-causal subsystems," *Automatica*, vol. 44, no. 11, pp. 2950 – 2953, 2008.